



Particle-In-Cell Based Beam Dynamics Simulations

Thomas Lau, E. Gjonaj and T. Weiland

EPAC, Luzern, 5-9.07.2004

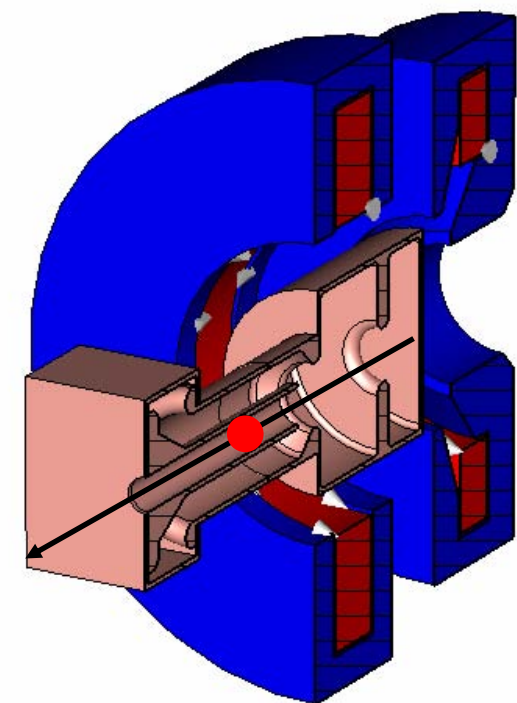
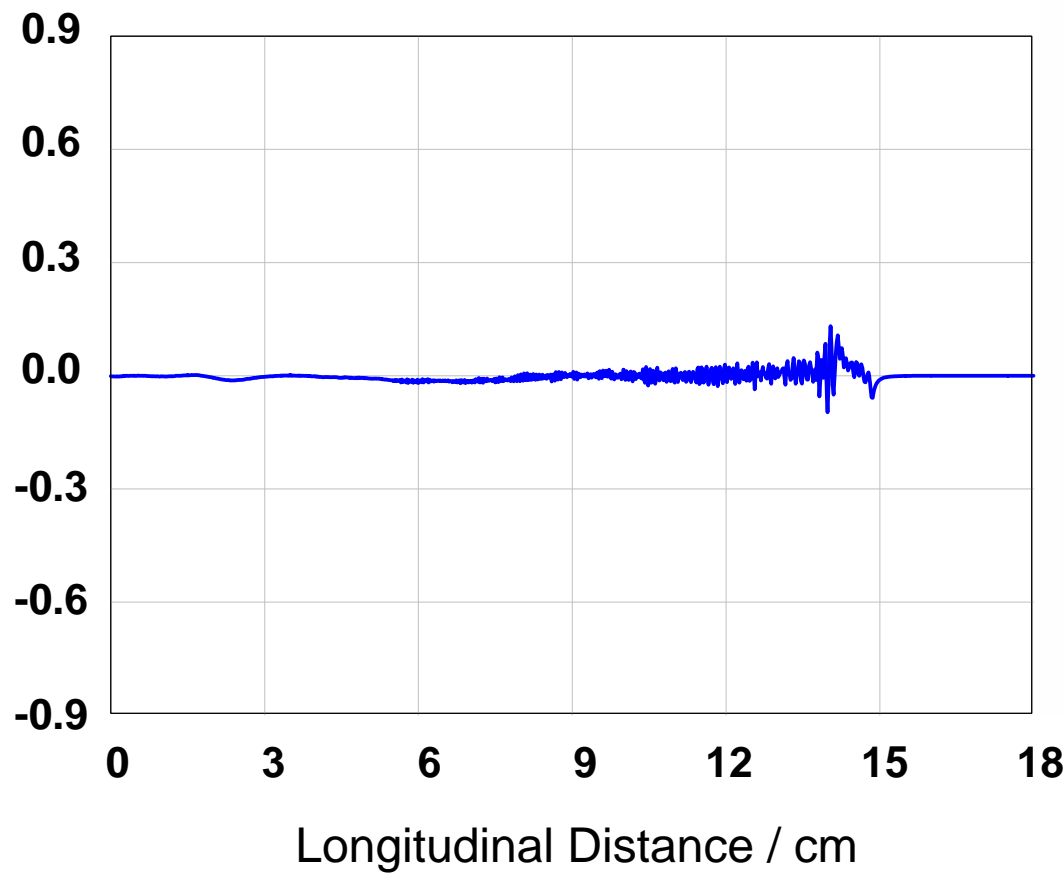


- Motivation
- Finite Integration Technique
 - Non Conformal
 - Conformal
- Noise Reduction
 - Splitting Scheme
 - Dissipative Scheme
- Analytical Benchmark
- Simulations
- Conclusions

- Motivation
- Finite Integration Technique
 - Non Conformal
 - Conformal
- Noise Reduction
 - Splitting Scheme
 - Dissipative Scheme
- Analytical Benchmark
- Simulations
- Conclusions

- Simulation of relativistic electron beams
- Bunch is much smaller than the geometry

Longitudinal Electric Field / MV/m



- Motivation
- Finite Integration Technique
 - Non Conformal
 - Conformal
- Noise Reduction
 - Splitting Scheme
 - Dissipative Scheme
- Analytical Benchmark
- Simulations
- Conclusions

Finite Integration Technique

Maxwell-Grid-Equations (Weiland, 1977)

Integral Maxwell Equations:

$$\oint_{\partial A} \vec{E} \cdot d\vec{s} = -\frac{\partial}{\partial t} \iint_A \vec{B} \cdot d\vec{A}$$

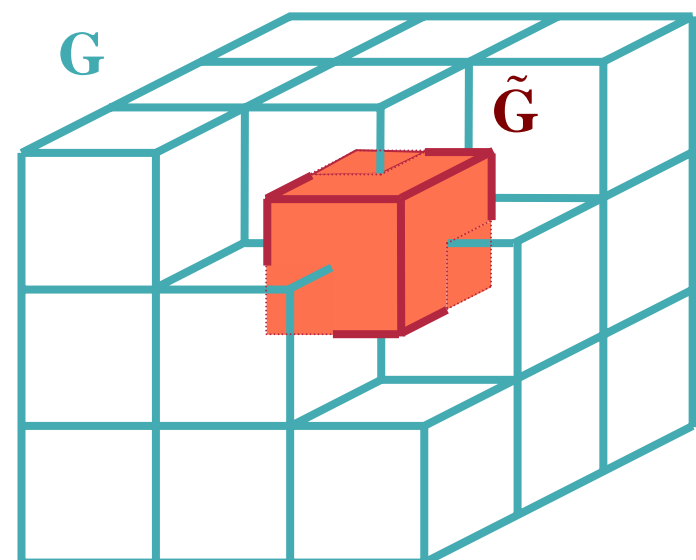
$$\oint_{\partial A} \vec{H} \cdot d\vec{s} = \iint_A \left(\frac{\partial}{\partial t} \vec{D} + \vec{J} \right) \cdot d\vec{A}$$

$$\iint_{\partial V} \vec{B} \cdot d\vec{A} = 0$$

$$\iint_{\partial V} \vec{D} \cdot d\vec{A} = \iiint_V \rho \, dV$$

Description by finite field *fluxes* and *voltages*

Grid-Dual-Grid Discretization:



$G \rightarrow$ Primary grid

$\tilde{G} \rightarrow$ Dual (orthogonal) grid

Finite Integration Technique

Maxwell-Grid-Equations (Weiland, 1977)

Integral Maxwell Equations:

$$\oint_{\partial A} \vec{E} \cdot d\vec{s} = -\frac{\partial}{\partial t} \iint_A \vec{B} \cdot d\vec{A}$$

$$\oint_{\partial A} \vec{H} \cdot d\vec{s} = \iint_A \left(\frac{\partial}{\partial t} \vec{D} + \vec{J} \right) \cdot d\vec{A}$$

$$\iint_{\partial V} \vec{D} \cdot d\vec{A} = \iiint_V \rho \, dV$$

$$\iint_{\partial V} \vec{B} \cdot d\vec{A} = 0$$



FIT Equations:

$$\mathbf{C}\hat{\mathbf{e}} = -\frac{d}{dt} \hat{\mathbf{b}}$$

$$\hat{\mathbf{C}}\hat{\mathbf{h}} = \frac{d}{dt} \hat{\mathbf{d}} + \hat{\mathbf{j}}$$

$$\tilde{\mathbf{S}}\hat{\mathbf{d}} = \mathbf{q}$$

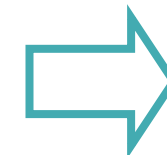
$$\mathbf{S}\hat{\mathbf{b}} = 0$$

- Exact mapping in grid-space
- Material equations needed:

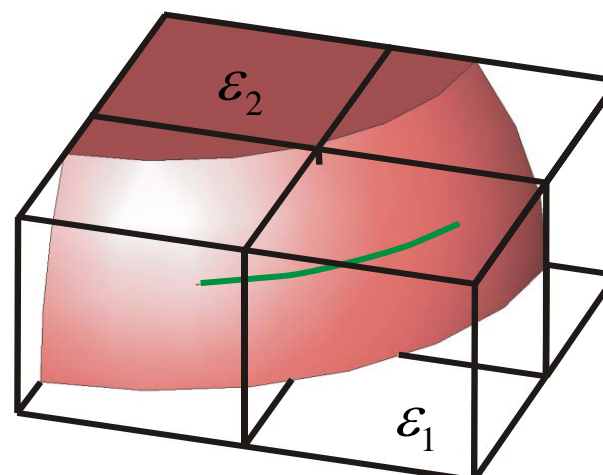
$$\hat{\mathbf{d}} \rightarrow \hat{\mathbf{e}}, \hat{\mathbf{b}} \rightarrow \hat{\mathbf{h}}$$

Material Operators. Staircase FIT

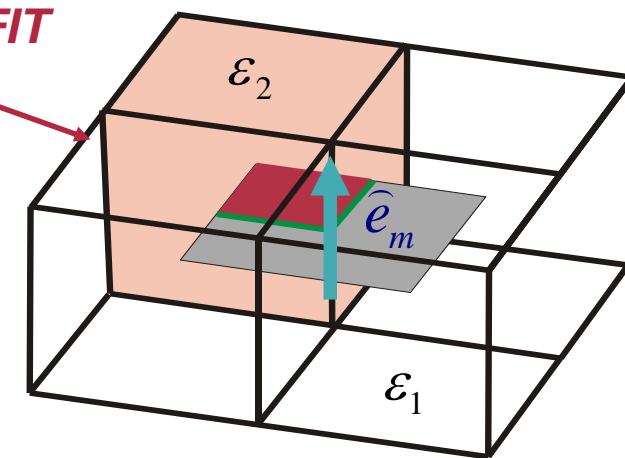
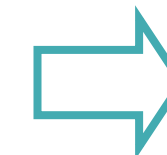
- Linear material operators
- Constructed by discretization
- Approximation depends on material operators only



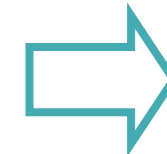
$$\begin{aligned}\vec{D} = \varepsilon \vec{E} &\Leftrightarrow \hat{\vec{d}} = \mathbf{M}_\varepsilon \hat{\vec{e}} \\ \mu \vec{H} = \vec{B} + \vec{M} &\Leftrightarrow \hat{\vec{h}} = \mathbf{M}_{\mu^{-1}} \hat{\vec{b}} + \hat{\vec{M}} \\ \vec{J} = \sigma \vec{E} + \vec{J}_s &\Leftrightarrow \hat{\vec{j}} = \mathbf{M}_\sigma \hat{\vec{e}} + \hat{\vec{j}}_s\end{aligned}$$



Staircasing FIT



- Diagonal, positive matrices for Cartesian grids

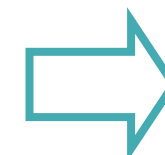


$$\hat{\vec{d}}_m \approx \left(\int_{A_m} \varepsilon \square dA / \int_{L_m} ds \right) \hat{\vec{e}}_m$$

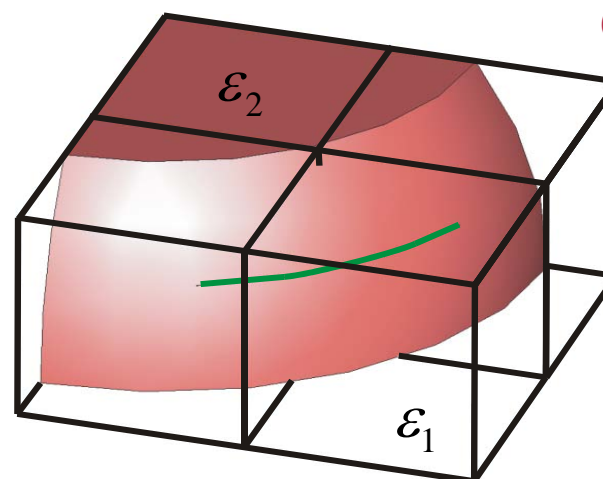
Finite Integration Technique

Material Operators. Conformal FIT

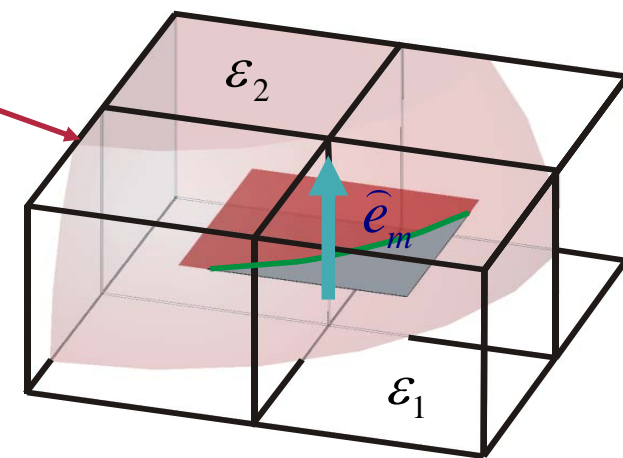
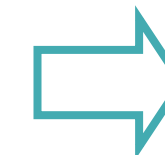
- Linear material operators
- Constructed by discretization
- Approximation depends on material operators only



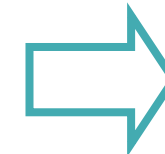
$$\begin{aligned}\vec{D} &= \varepsilon \vec{E} & \Leftrightarrow \hat{\mathbf{d}} &= \mathbf{M}_\varepsilon \hat{\mathbf{e}} \\ \vec{H} &= \mu \vec{B} & \Leftrightarrow \hat{\mathbf{h}} &= \mathbf{M}_\mu \hat{\mathbf{b}} \\ \vec{J} &= \sigma \vec{E} + \vec{J}_s & \Leftrightarrow \hat{\mathbf{j}} &= \mathbf{M}_\sigma \hat{\mathbf{e}} + \hat{\mathbf{j}}_s\end{aligned}$$



Conformal FIT



- Diagonal, positive matrices for Cartesian grids



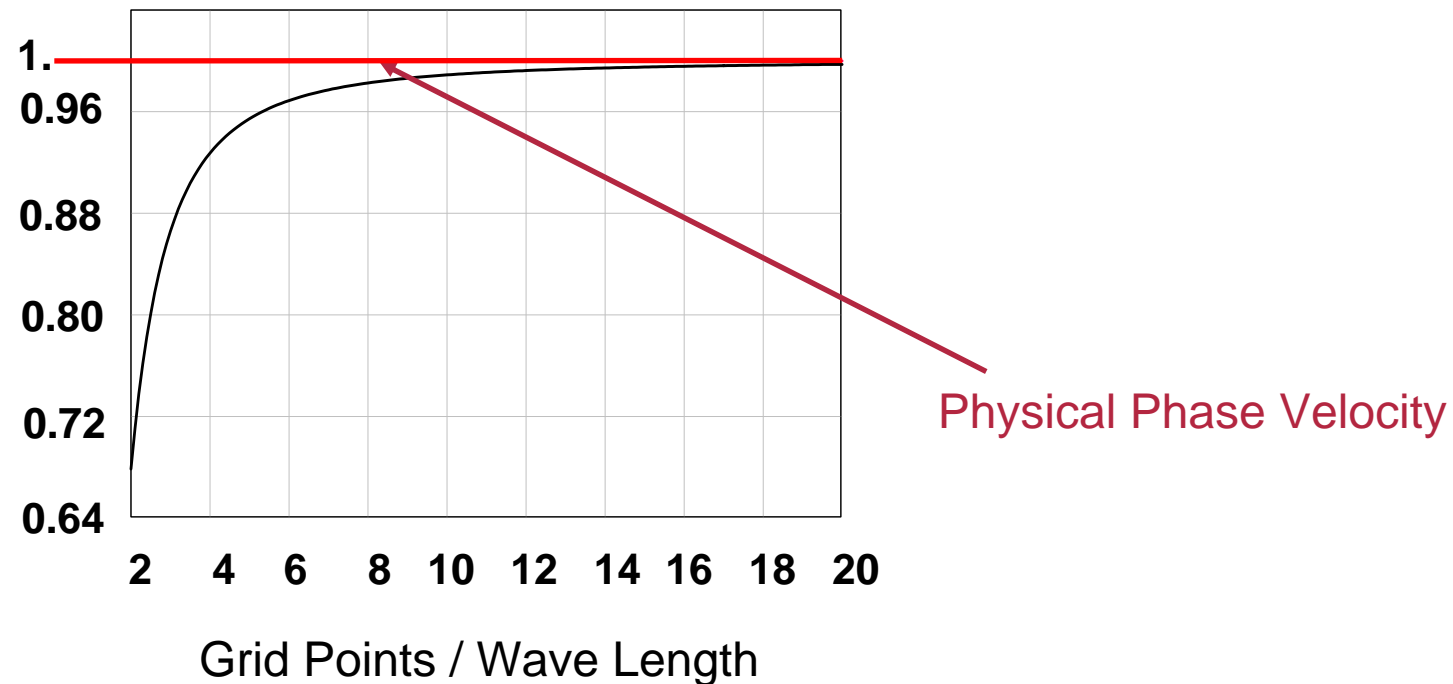
$$\hat{d}_m \approx \left(\int_{A_m} \varepsilon \square dA / \int_{L_m} ds \right) \hat{e}_m$$

- Motivation
- Finite Integration Technique
 - Non Conformal
 - Conformal
- Noise Reduction
 - Splitting Scheme
 - Dissipative Scheme
- Analytical Benchmark
- Simulations
- Conclusions

Leap-Frog Scheme

$$\begin{pmatrix} \hat{\mathbf{h}}^{(n+1)} \\ \hat{\mathbf{e}}^{(n+3/2)} \end{pmatrix} = \begin{pmatrix} 1 & -\Delta t \cdot \mathbf{M}_{\mu^{-1}} \mathbf{C} \\ \Delta t \cdot \mathbf{M}_{\varepsilon^{-1}} \tilde{\mathbf{C}} & 1 + \Delta t^2 \mathbf{M}_{\varepsilon^{-1}} \tilde{\mathbf{C}} \mathbf{M}_{\mu^{-1}} \mathbf{C} \end{pmatrix} \begin{pmatrix} \hat{\mathbf{h}}^{(n)} \\ \hat{\mathbf{e}}^{(n+1/2)} \end{pmatrix} + \Delta t \begin{pmatrix} 0 \\ \mathbf{M}_{\varepsilon^{-1}} \tilde{\mathbf{j}}_s \end{pmatrix}$$

Discrete Phase Velocity



Transversal Current Adjustment (TCA)

- Introduces an **artificial damping** of short wavelengths
- Formulation as Curl Curl operator ensures that neither new electric nor new magnetic charges are created by the artificial damping term

Artificial Damping Term

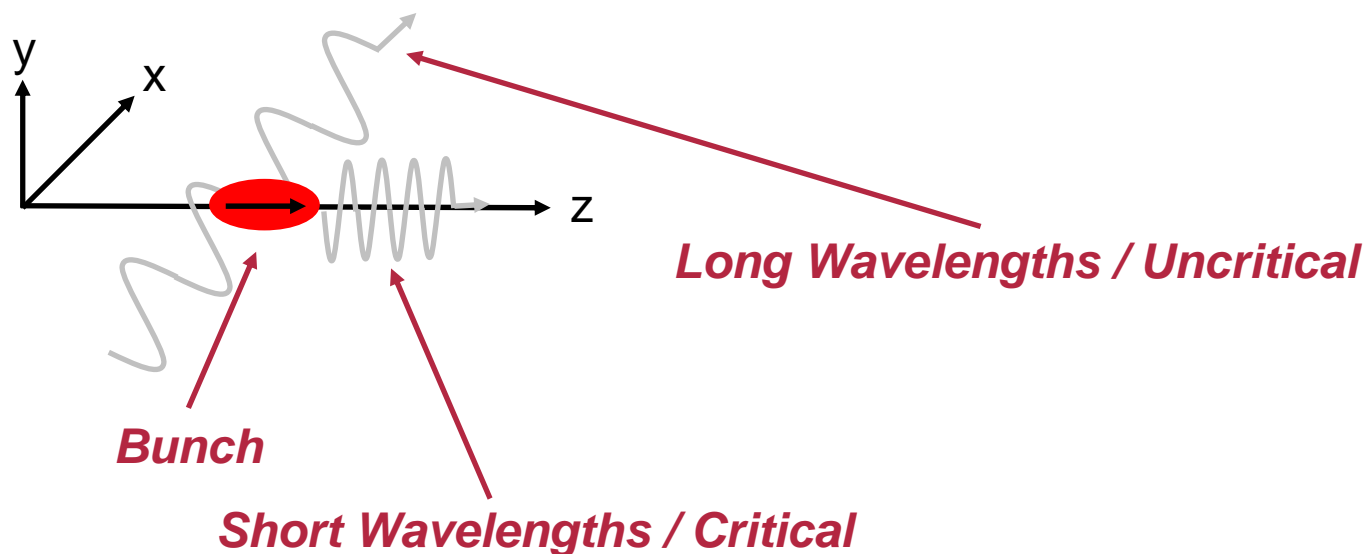
$$\begin{pmatrix} \hat{\mathbf{h}}^{(n+1)} \\ \hat{\mathbf{e}}^{(n+3/2)} \end{pmatrix} = \begin{pmatrix} \mathbf{1} + \alpha \Delta t^2 \mathbf{M}_{\varepsilon^{-1}} \tilde{\mathbf{C}} \mathbf{M}_{\mu^{-1}} \mathbf{C} & -\Delta t \cdot \mathbf{M}_{\mu^{-1}} \mathbf{C} \\ \Delta t \cdot \mathbf{M}_{\varepsilon^{-1}} \tilde{\mathbf{C}} & \mathbf{1} + \Delta t^2 \mathbf{M}_{\varepsilon^{-1}} \tilde{\mathbf{C}} \mathbf{M}_{\mu^{-1}} \mathbf{C} \end{pmatrix} \begin{pmatrix} \hat{\mathbf{h}}^{(n)} \\ \hat{\mathbf{e}}^{(n+1/2)} \end{pmatrix} + \Delta t \begin{pmatrix} 0 \\ \mathbf{M}_{\varepsilon^{-1}} \tilde{\mathbf{j}}_s^{(n+1)} \end{pmatrix}$$



Transversal Current Adjustment (TCA)

- Easy to implement
- Has a variable damping parameter
 - The optimal value is problem dependent
- Decreases the stability limit of the Leap-Frog method
 - The time step has to be reduced
- There is minimal numerical overhead compared to the Leap-Frog method

Longitudinal Transversal Operator Splitting



Split the Maxwell equations, with respect to space, into a transversal and a longitudinal part

Longitudinal-Transversal Strang Splitting

$$\begin{pmatrix} \hat{\mathbf{h}}^{(*)} \\ \hat{\mathbf{e}}^{(*)} \end{pmatrix} = \begin{pmatrix} 1 & -\frac{\Delta t}{2} \cdot \mathbf{M}_{\mu^{-1}} \tilde{\mathbf{C}}_T \\ \frac{\Delta t}{2} \cdot \mathbf{M}_{\varepsilon^{-1}} \tilde{\mathbf{C}}_T & 1 \end{pmatrix} \begin{pmatrix} \hat{\mathbf{h}}^{(n)} \\ \hat{\mathbf{e}}^{(n+1/2)} \end{pmatrix} + \frac{\Delta t}{2} \begin{pmatrix} 0 \\ \mathbf{M}_{\varepsilon^{-1}} \tilde{\mathbf{j}}_s^{(n+1)} \end{pmatrix}$$

*Transversal Update
First Half Step*

$$\begin{pmatrix} \hat{\mathbf{h}}^{(**)} \\ \hat{\mathbf{e}}^{(**)} \end{pmatrix} = \begin{pmatrix} 1 & -\Delta t \cdot \mathbf{M}_{\mu^{-1}} \tilde{\mathbf{C}}_L \\ \Delta t \cdot \mathbf{M}_{\varepsilon^{-1}} \tilde{\mathbf{C}}_L & 1 \end{pmatrix} \begin{pmatrix} \hat{\mathbf{h}}^{(*)} \\ \hat{\mathbf{e}}^{(*)} \end{pmatrix}$$

Longitudinal Update

$$\begin{pmatrix} \hat{\mathbf{h}}^{(n+1)} \\ \hat{\mathbf{e}}^{(n+3/2)} \end{pmatrix} = \begin{pmatrix} 1 & -\frac{\Delta t}{2} \cdot \mathbf{M}_{\mu^{-1}} \tilde{\mathbf{C}}_T \\ \frac{\Delta t}{2} \cdot \mathbf{M}_{\varepsilon^{-1}} \tilde{\mathbf{C}}_T & 1 \end{pmatrix} \begin{pmatrix} \hat{\mathbf{h}}^{(**)} \\ \hat{\mathbf{e}}^{(**)} \end{pmatrix} + \frac{\Delta t}{2} \begin{pmatrix} 0 \\ \mathbf{M}_{\varepsilon^{-1}} \tilde{\mathbf{j}}_s^{(n+1)} \end{pmatrix}$$

*Transversal Update
Second Half Step*



Longitudinal-Transversal Strang Splitting

- Uses the largest time step possible for relativistic beams, the Courant time step
- Is 2 times more expensive than the Leap-Frog method, but the time step is 1.7 times greater
- Has zero dispersion along the beam axis at the Courant time step
- Is still second order accurate in space and time
- The splitting error creates magnetical and electrical charges
 - This seems not to be a problem in practical calculations

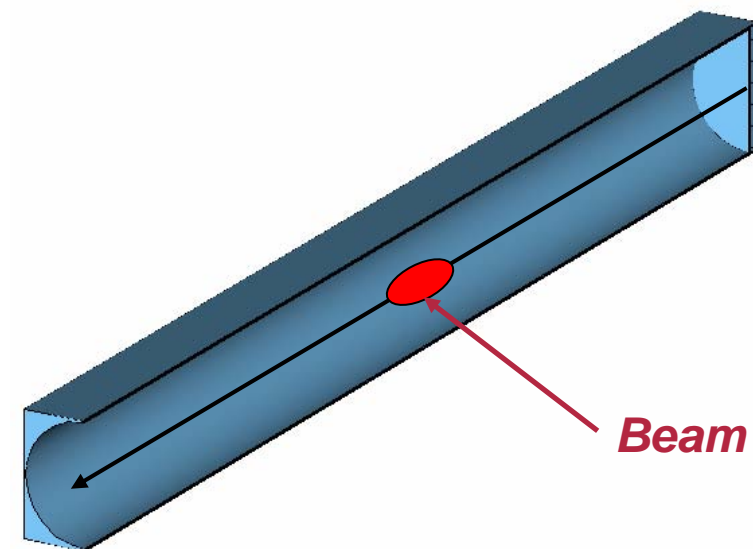


- Motivation
- Finite Integration Technique
 - Non Conformal
 - Conformal
- Noise Reduction
 - Splitting Scheme
 - Dissipative Scheme
- Analytical Benchmark
- Simulations
- Conclusions

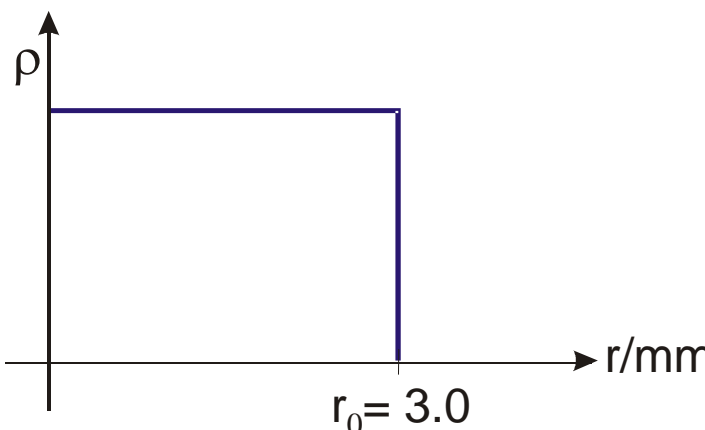
Analytical Benchmark

Bunch Parameters:

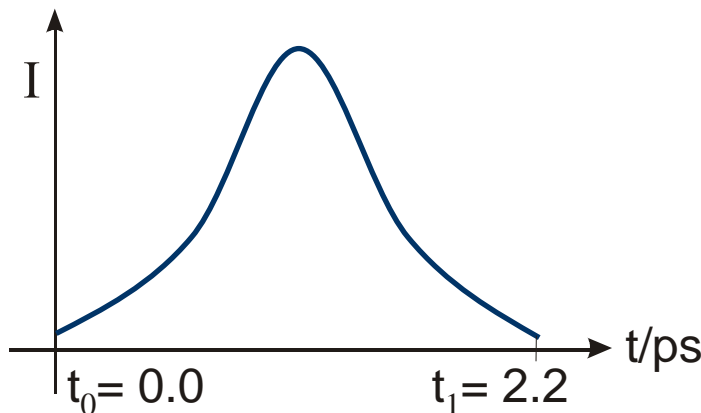
Q_{Bunch}	-1 / nC
β_{Bunch}	0.9
r_{Bunch}	3.0 / mm
l_{Bunch}	6.0 / mm
r_{Tube}	20.0 / mm



Radial Distribution:

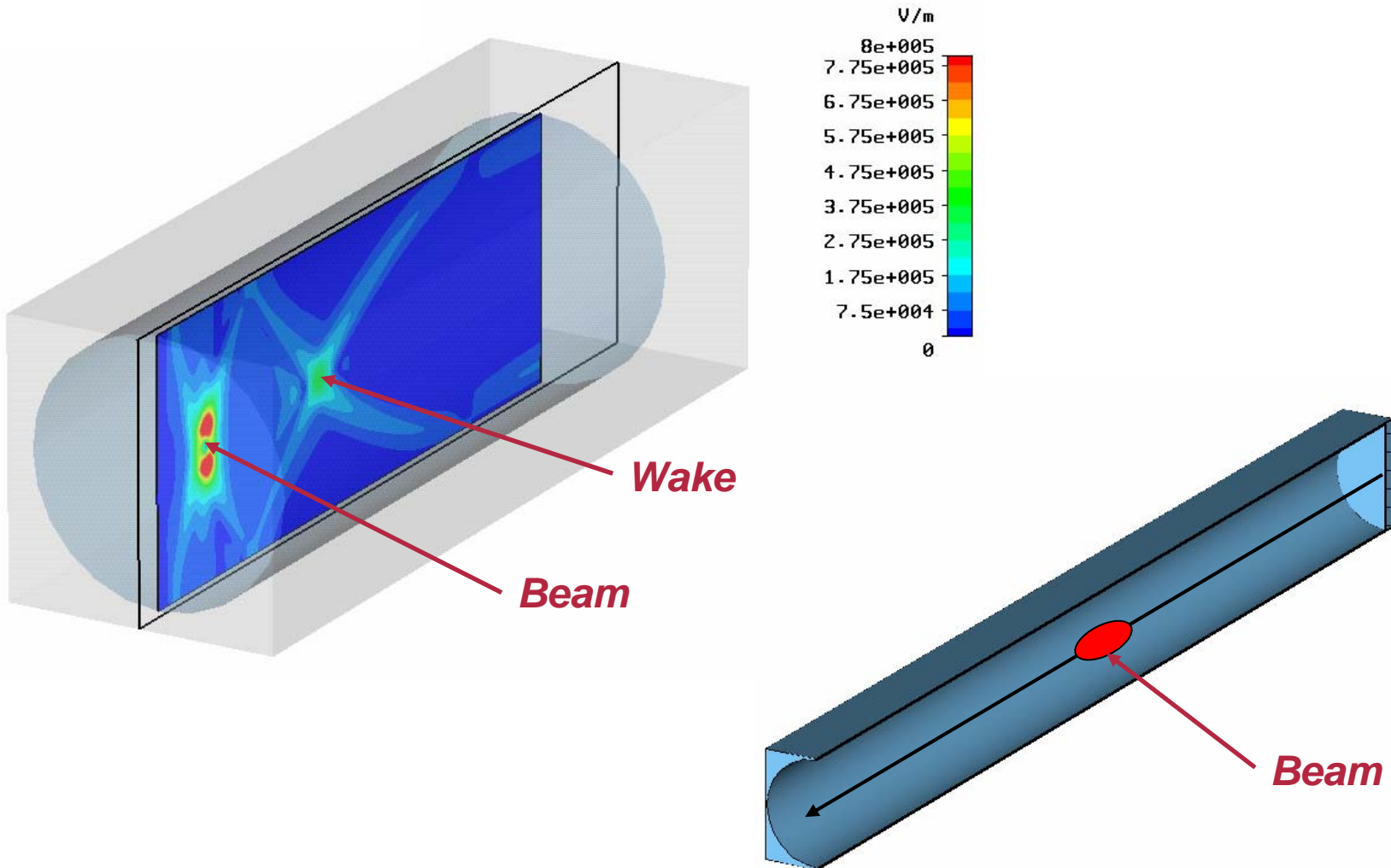


Gaussian Time Distribution:



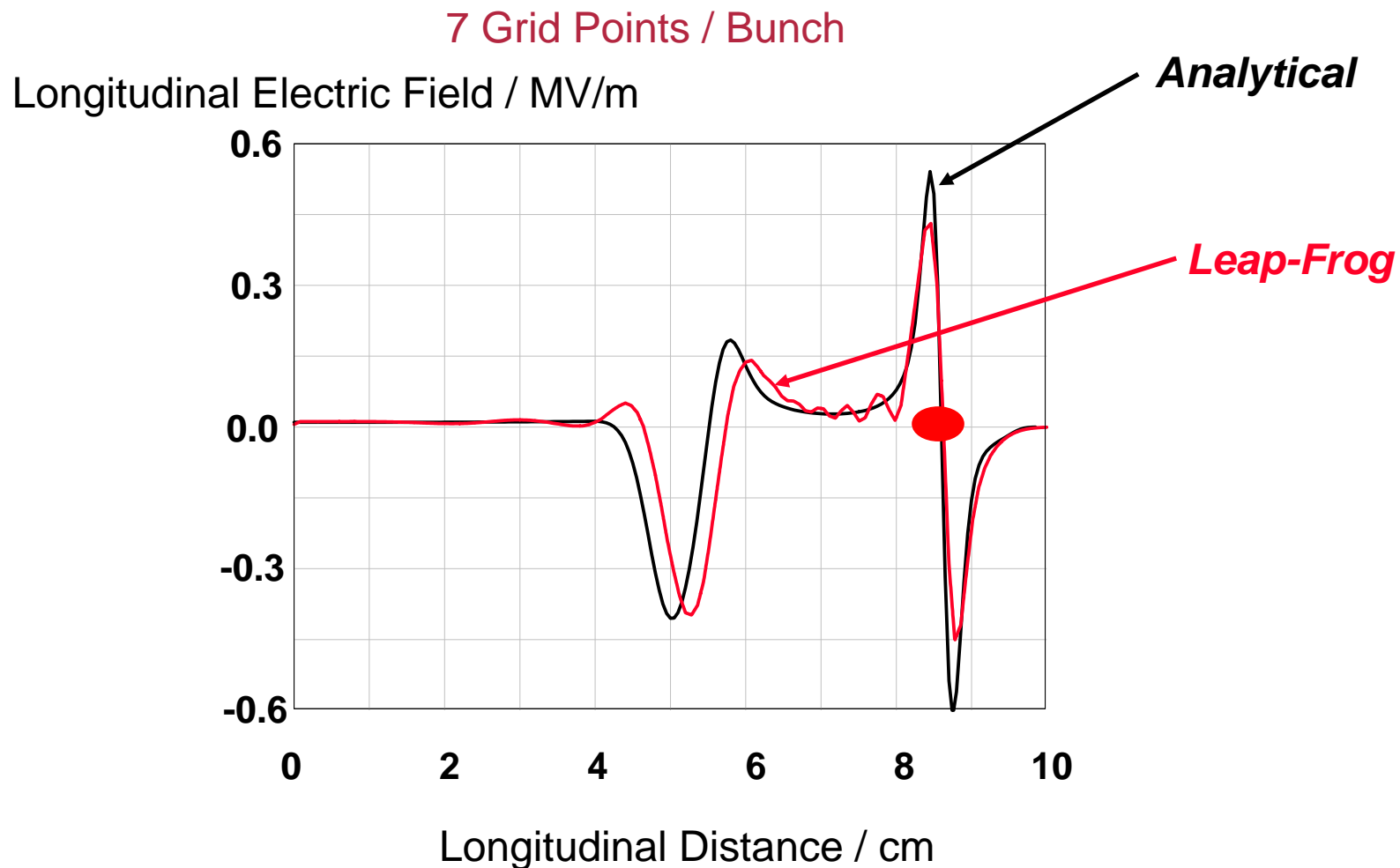
Analytical Benchmark

Absolute Value of Electrical Field in the Waveguide



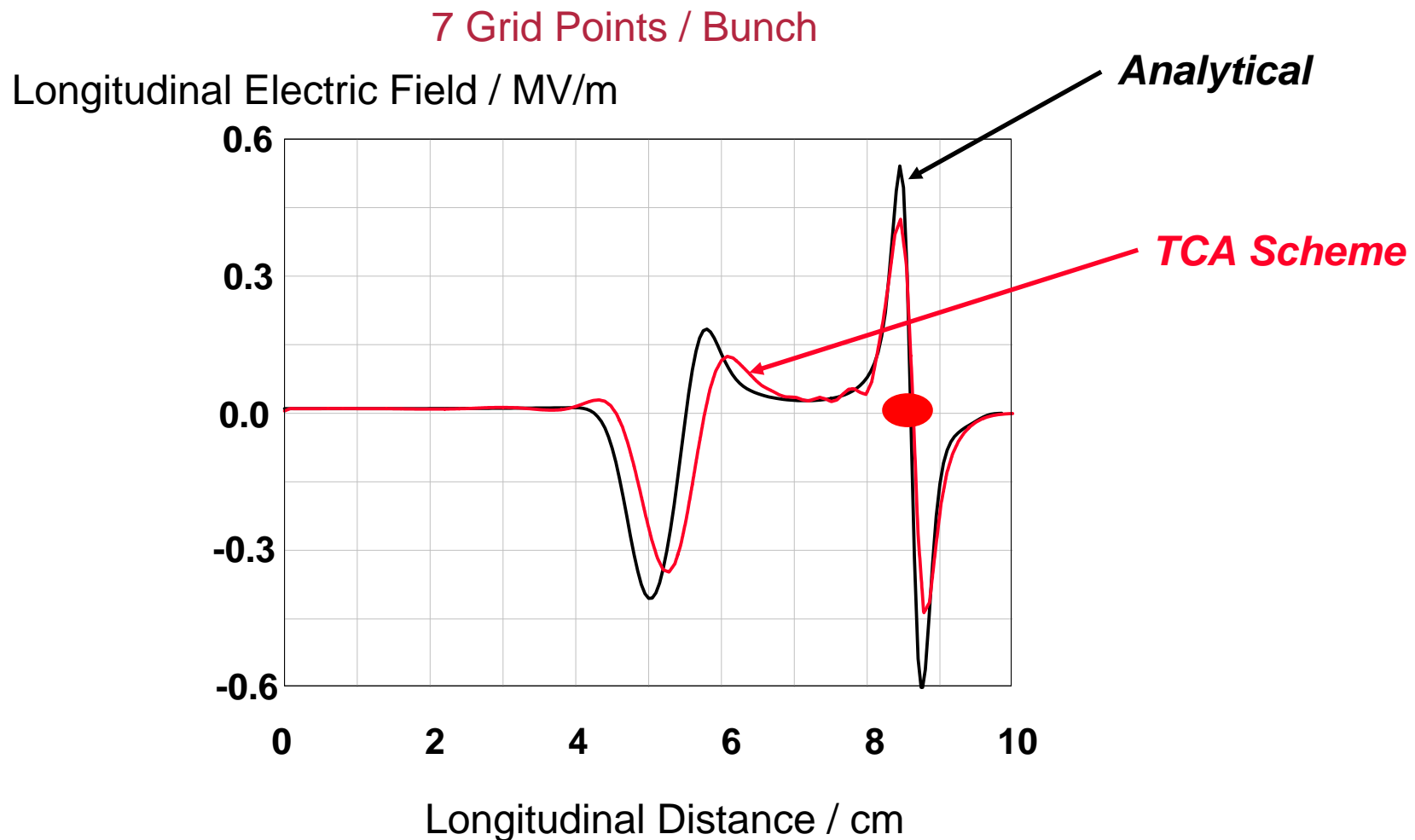
Analytical Benchmark

Longitudinal Electric Field on the Beam Axis



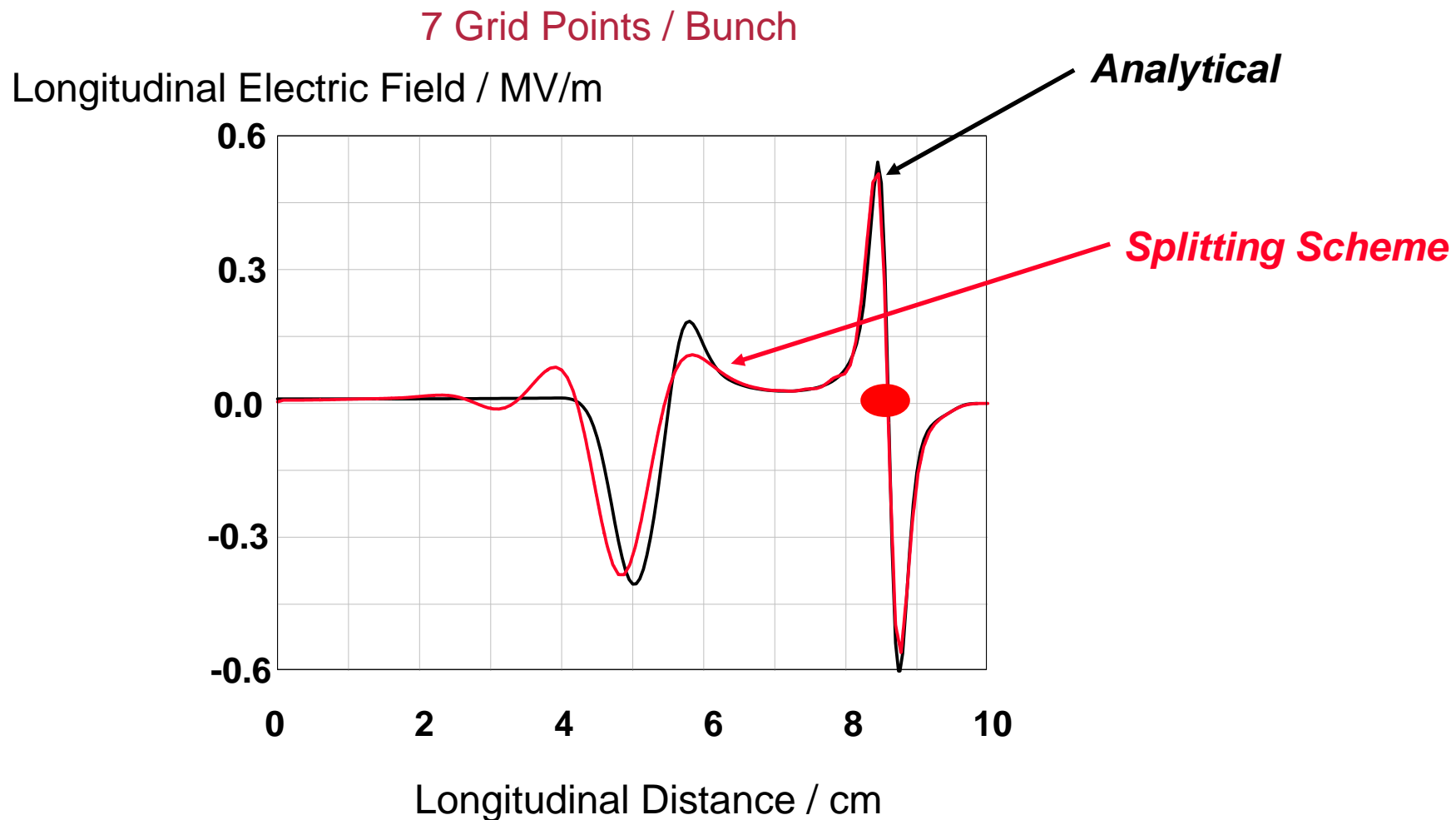
Analytical Benchmark

Longitudinal Electric Field on the Beam Axis



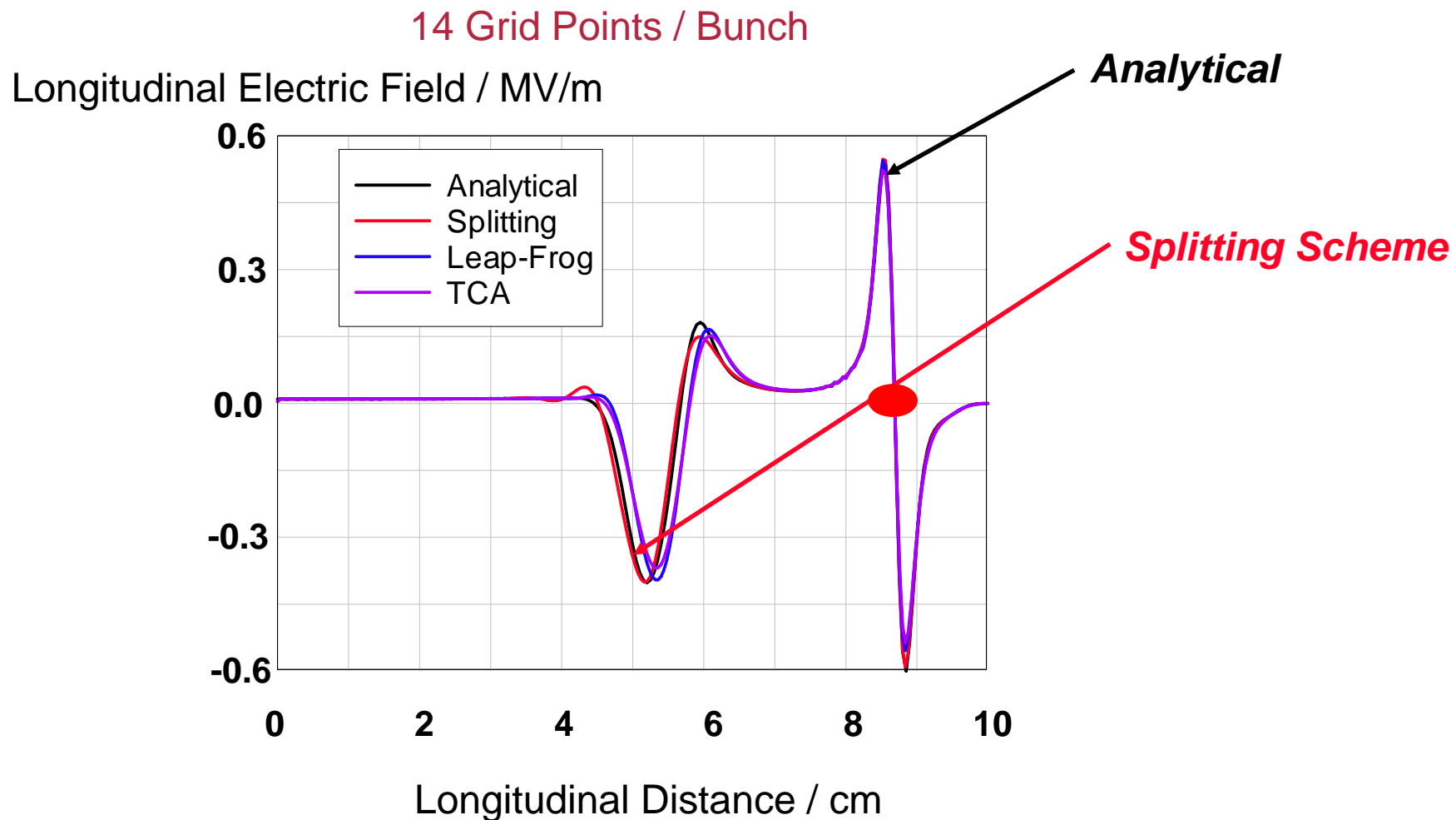
Analytical Benchmark

Longitudinal Electric Field on the Beam Axis



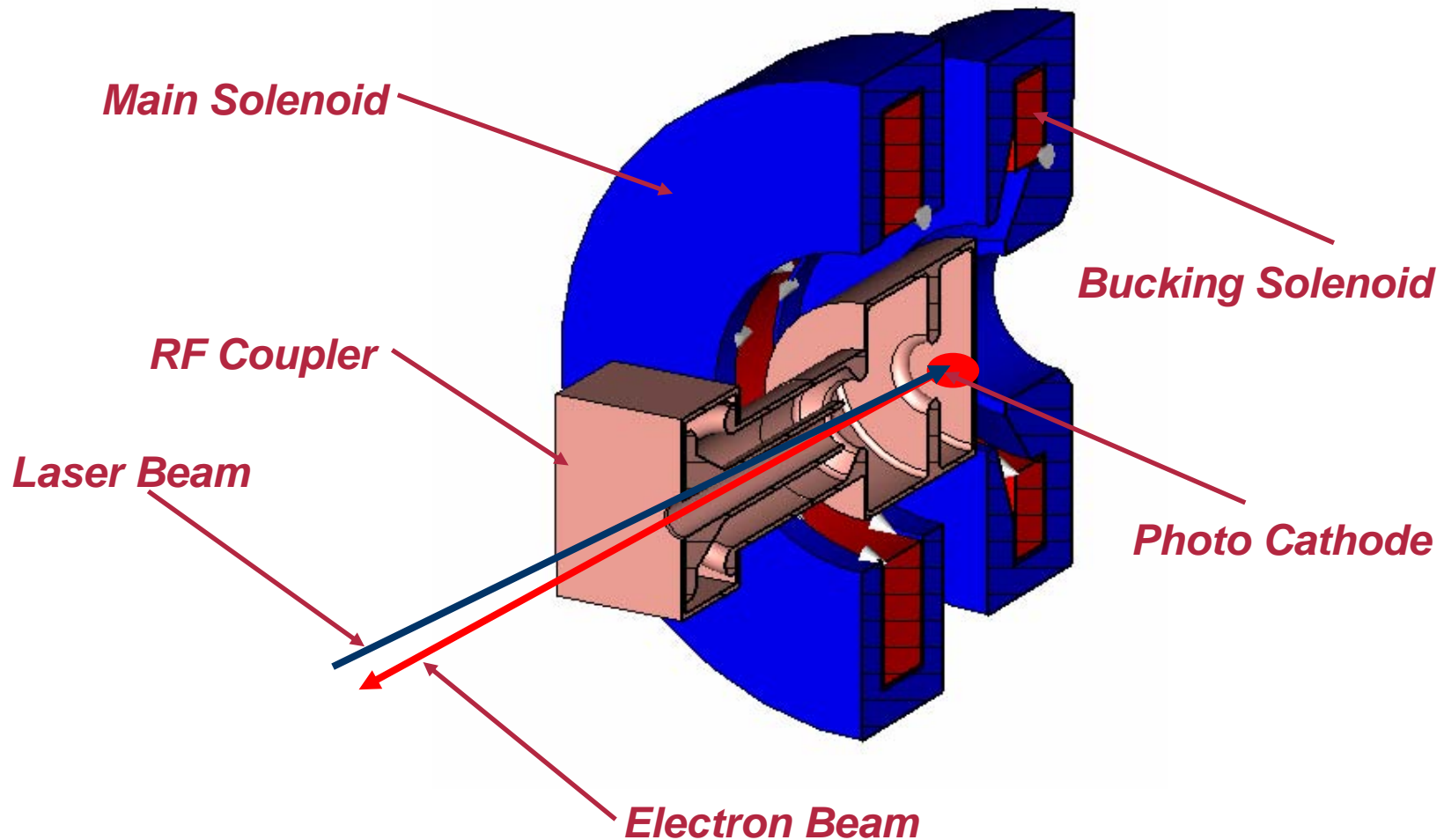
Analytical Benchmark

Longitudinal Electric Field on the Beam Axis

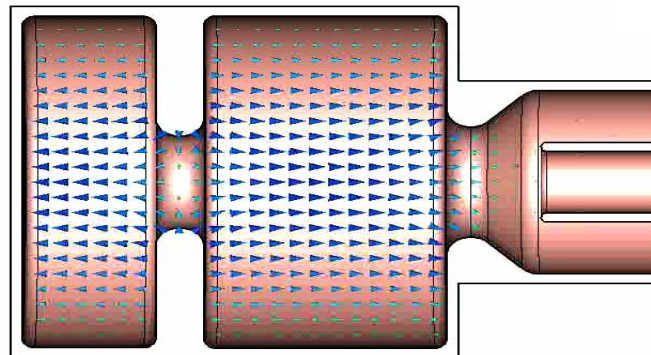


- Motivation
- Finite Integration Technique
 - Non Conformal
 - Conformal
- Noise Reduction
 - Splitting Scheme
 - Dissipative Scheme
- Analytical Benchmark
- **Simulations**
- Conclusions

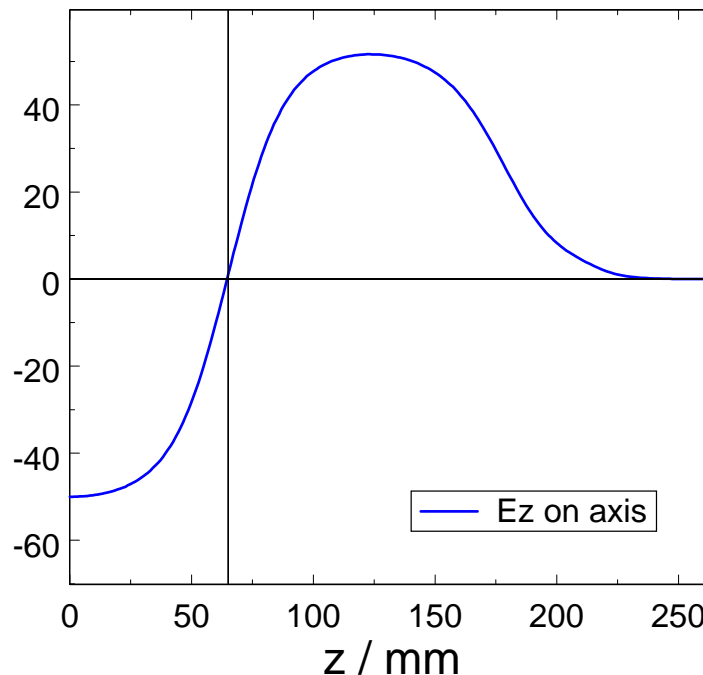
PITZ RF-Gun



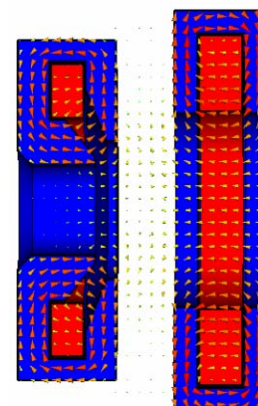
Cavity:



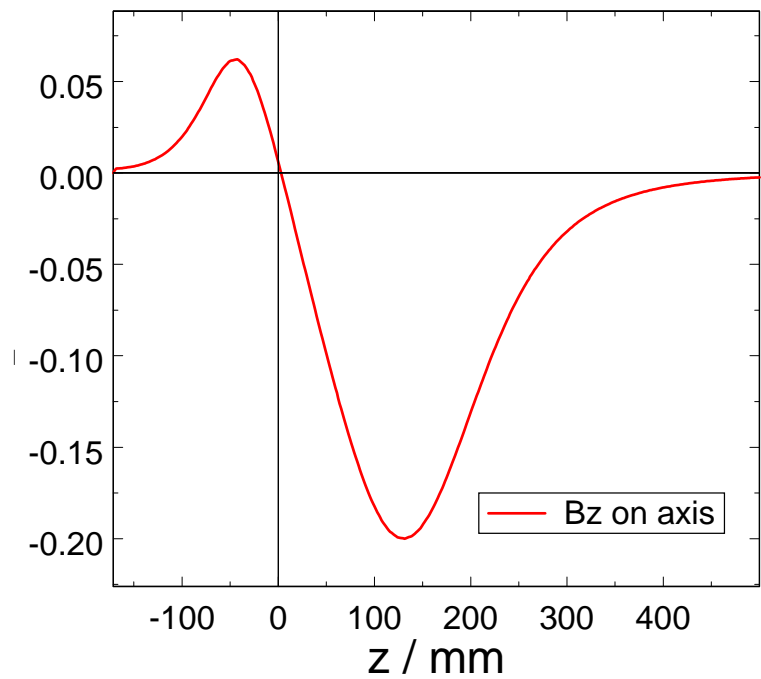
Longitudinal Electric Field / MV/m



Solenoids:

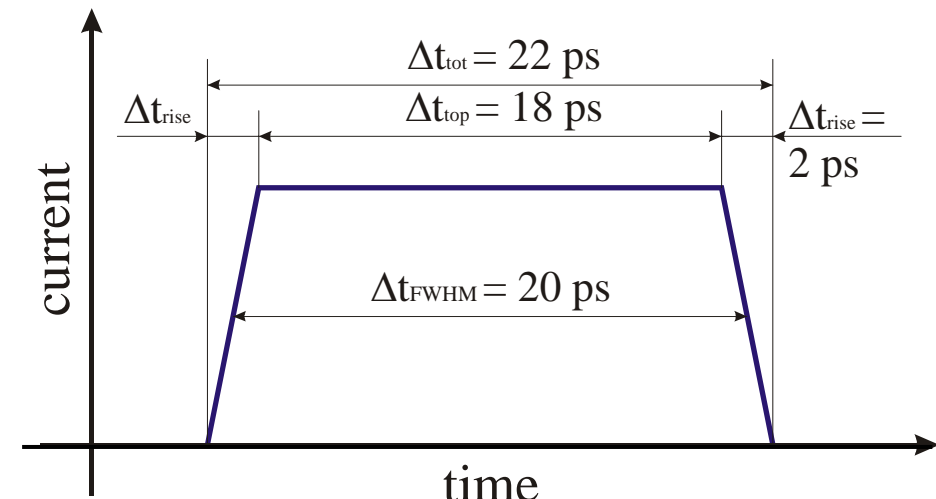
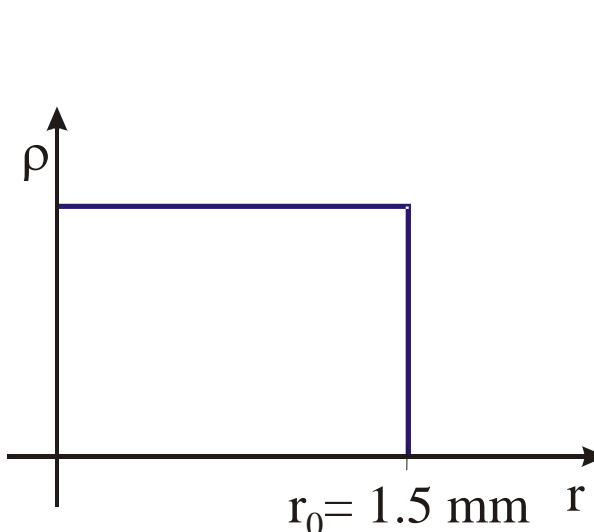


Longitudinal Magnetic Field / Tesla



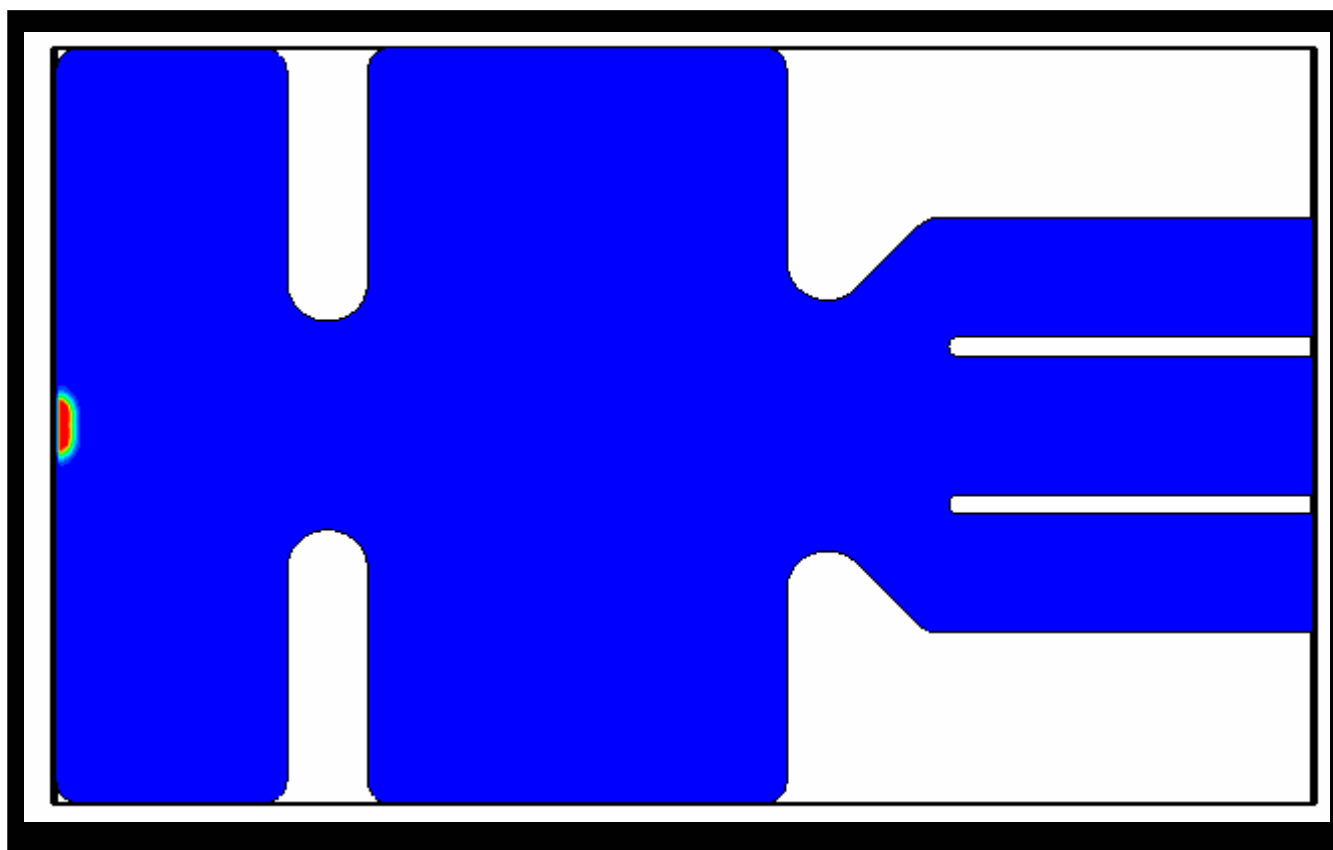
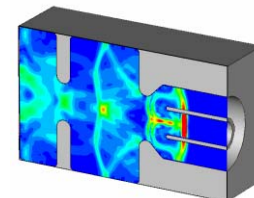
Bunch Parameters:

bunch radius	$r_0 = 1.5 \text{ mm}$
bunch charge	$q = -1 \text{ nC}$
bunch length	$\Delta t_{FWHM} = 20 \text{ ps}$
rise/fall time	$\Delta t_{rise} = 2 \text{ ps}$
reference phase	$\varphi_0 = -47.4^\circ$
field at cathode	$E_{cath} = -40.0 \text{ MV/m}$



Electrical Space Charge Field in the PITZ - Cavity

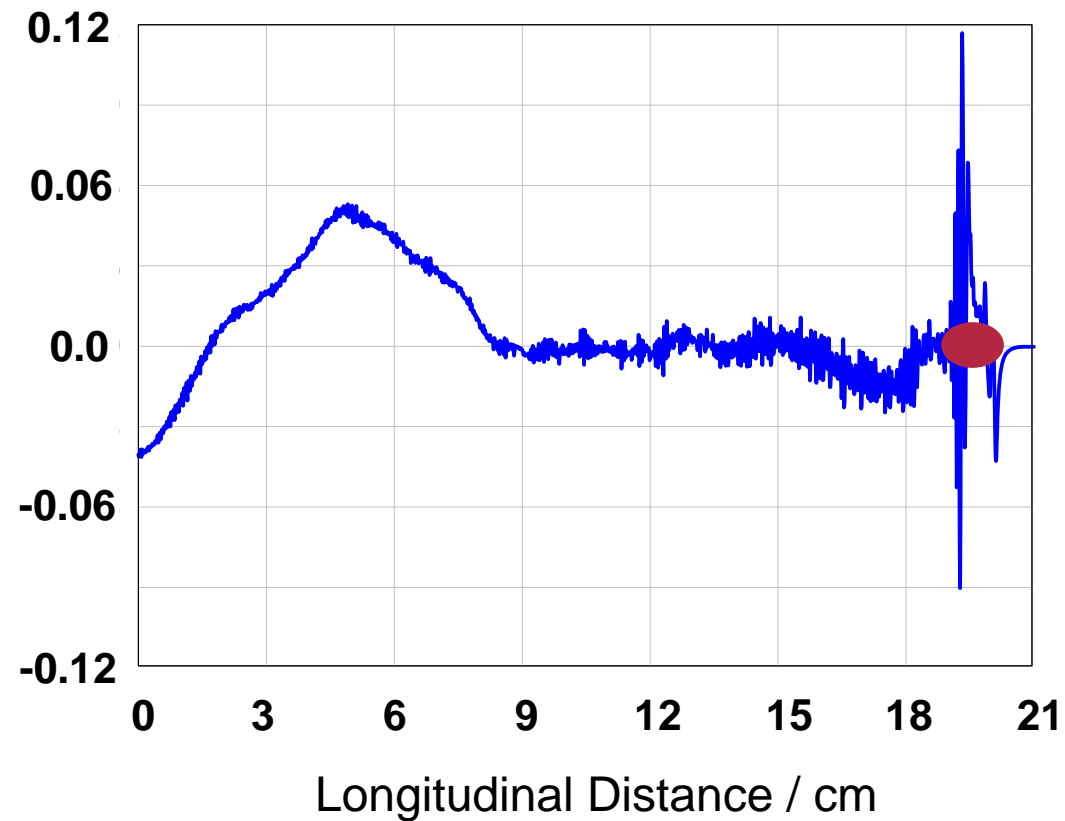
- RF fields are precalculated
- Fully 3D simulation



Longitudinal Electrical Field on the Beam Axis

Leap-Frog Scheme

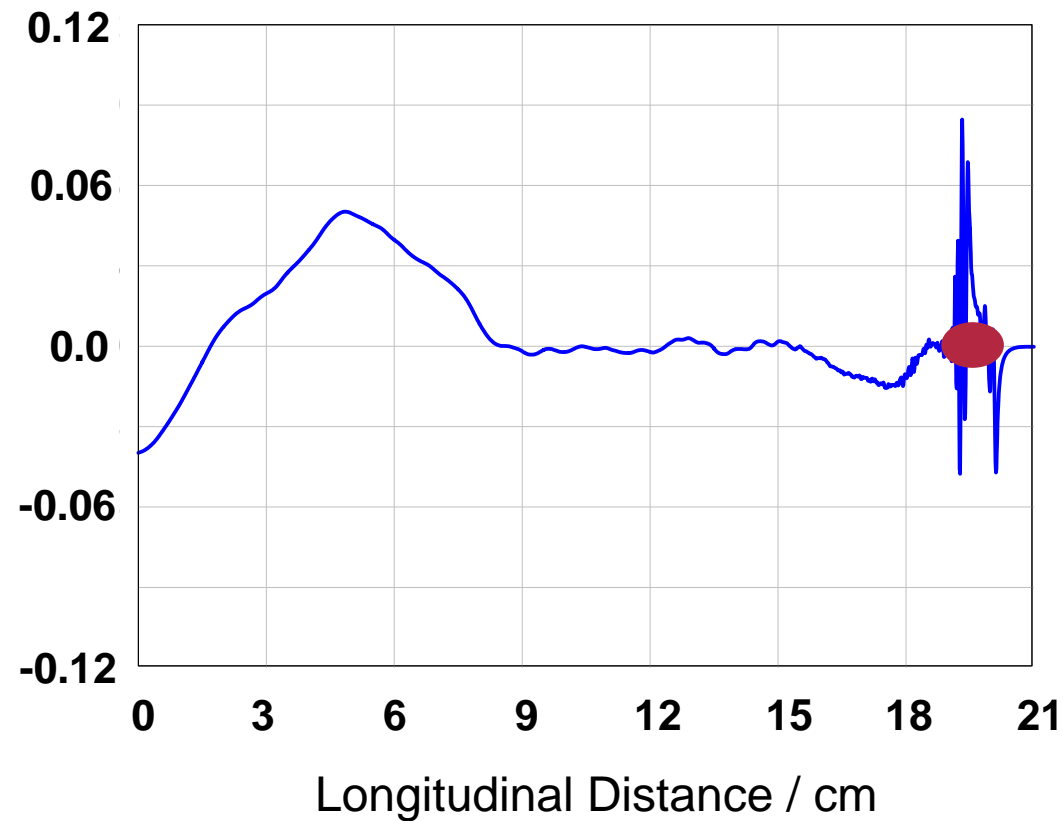
Longitudinal Electric Field / MV/m



Longitudinal Electrical Field on the Beam Axis

TCA Scheme

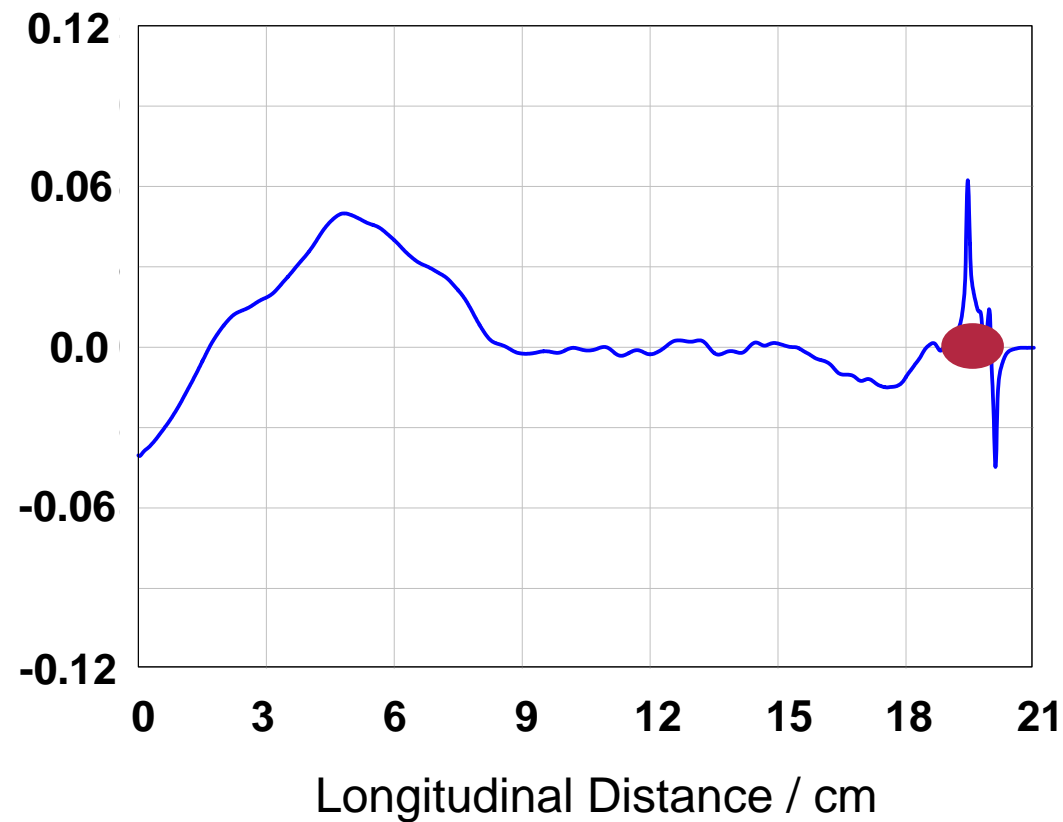
Longitudinal Electric Field / MV/m



Longitudinal Electrical Field on the Beam Axis

Splitting Scheme

Longitudinal Electric Field / MV/m



- Motivation
- Finite Integration Technique
 - Non Conformal
 - Conformal
- Noise Reduction
 - Splitting Scheme
 - Dissipative Scheme
- Analytical Benchmark
- Simulations
- **Conclusions**



Conclusions

- The conventional method has a large numerical error
- Large structures with short bunches cannot be simulated.

S. Schnepp – Poster THPLT037 – „Investigation of Numerical Noise in PIC-codes“

S. Setzer – Poster WEPLT061 – „Influence of Beam Tube Obstacles on the Emittance of the PITZ Photoinjector“

E. Gjonaj – Poster THPLT035 – „Development of a 3D-Gun-Code based on a Charge Conserving Algorithm“

- Full 3D simulations of e.g. modern high brightness electron sources at in reach

Thank You for the Attention